Controlling polymer properties through the shape of the molecular-weight distribution

Dillon T. Gentekos, Renee J. Sifri and Brett P. Fors *

Abstract | The manipulation of a polymer's properties without altering its chemical composition is a major challenge in polymer chemistry, materials science and engineering. Although variables such as chemical structure, branching, molecular weight and dispersity are routinely used to control the architecture and physical properties of polymers, little attention is given to the often profound effect of the breadth and shape of the molecular-weight distribution (MWD) on the properties of polymers. Synthetic strategies now make it possible to explore the importance of parameters such as skew and the higher moments of the MWD function beyond the average and standard deviation. In this Review, we describe early accounts of the effect of MWD shape on polymer properties; discuss synthetic strategies for controlling MWD shape; describe current endeavours to understand the influence of MWD shape on rheological and mechanical properties and phase behaviour; and provide insight into the future of using MWDs in the design of polymeric materials.

The molecular-weight distributions (MWDs) of polymers have a striking impact over their properties, from processability and mechanical strength to nearly all aspects of morphological phase behaviour[1–10]. The most common molecular parameter used to describe polymer MWDs is the dispersity ($Đ$) — the normalized standard deviation of chain sizes in a polymer sample, which is defined as the ratio of the weight-average molar mass (M_w) to the number-average molar mass (M_n). A more detailed description of these terms is provided in BOXES 1,2.

The parameter $Đ$ has been used to manipulate the properties of polymeric materials[11–19]. However, $Đ$ is an incomplete representation of a polymer's true distribution because it describes only the relative breadth of a MWD and contains no information regarding the precise composition of polymer chain lengths[13,14] (BOX 1). For this reason, interest has arisen in using the entire distribution of masses of a polymer sample to dictate its function. In theory, this would allow for limitless variation of the distribution function. However, until recently, this avenue of controlling polymer structure and function remained largely unexplored, owing to the lack of methods for controlling the absolute composition of chain lengths in a polymer sample.

In this Review, we explore advances in the synthetic control of polymer MWD shape, from temporally controlled polymer initiation and termination to reactant feeds in continuous-flow setups that produce homopolymers and block copolymers with precisely defined MWD shapes and compositional gradients. We also highlight the impact of polymer MWD shape on polymer properties, from tensile strength and rheological behaviour (for example, viscosity) to a variety of morphological characteristics for block copolymer self-assembly, such as domain spacing, and the position of morphological phase boundaries.

Synthetic control of MWD shape

The properties of a polymer depend on the breadth and shape of the MWD in the final polymeric material[5,20] and, as a result, a number of approaches have been developed to control polymer $Đ$. Owing to the synthetic difficulty in controlling both the molar mass averages and the MWD breadth in a one-pot setup, early studies used post-polymerization blending strategies to tailor the MWD composition[21–26]. However, this process requires the synthesis of multiple polymers under highly controlled conditions and results in multimodal MWDs. Although these studies provided insight into the influence of MWD on polymer properties, such heterogeneous molar mass compositions are unsuitable for some applications, owing to the potential for undesirable macrophase separation[21,22]. Therefore, systems that produce polymers with continuous monomodal MWDs in a one-reactor setup are more desirable. Uncontrolled polymerization is one such synthetic strategy for producing monomodal MWDs with large

Department of Chemistry and Chemical Biology, Cornell University, Ithaca, NY, USA.

**e-mail: bpf46@cornell.edu*

https://doi.org/10.1038/s41578-019-0138-8

breadths[27–29]. Although this approach has proven useful in generating polymers with $Đ \approx 2$, it grants little control over M_n or the shape of the resultant MWD. This issue has been circumvented by leveraging polymer chain growth kinetics in radical, ring-opening and anionic polymerizations to prepare polymers with controllable dispersities[30–33]. For example, controlled atom-transfer radical coupling (ATRC) has allowed for changes in the MWD breadth, as well as the ability to achieve both monomodal and multimodal MWDs[34]. However, ATRC is limited in its monomer scope and lacks the precise control needed to obtain exact MWD shapes. Furthermore, mathematical models of catalyst-transfer polycondensation polymerizations have been studied as a means of deviating from ideal Poisson behaviour[35]. Although these models may provide the foundation for gaining control over $Đ$ and the distribution function, this model is specific to only a few mechanisms based on polymer kinetics. Alternatively, to tune the polymer $Đ$, researchers have developed an organocatalytic process that takes advantage of monomer mixtures to manipulate the dispersity of any block of a block copolymer[36].

Recent work has made strides towards MWD control by deep reinforcement learning to simulate the production of a vast repertoire of MWDs in atom-transfer radical polymerization (ATRP)[37]. Reinforcement learning is a machine-learning technique that allows a system to react with its environment and make decisions based on reward points. Whenever the system takes an action that moves it closer to the desired goal, it receives a reward, thus providing a guide to reach the final goal. In this case for ATRP, the reinforcement learning model allows the system to take actions, such as changing the amount of monomer, initiator or solvent, to achieve a desired MWD. These numerical simulations yielded reactor-control policies that should afford targeted MWD shapes, from monomodal distributions with deviating $Đ$ values to multimodal MWDs.

Although the aforementioned approaches can be used to modify $Đ$ with high fidelity, they are not a means of governing the precise composition or shape of the polymer MWD. In contrast with strategies for modifying $Đ$, few have been developed for customizing the MWD shape. In early work, control over the MWD shape was reported in anionic polymerization of styrene through oscillating monomer and alkyllithium initiator feed rates in continuous-flow reactors[38,39]. This method monitors the MWD in real time and uses mathematical modelling to alter the flow rates of the reacting species to achieve the desired MWD. Although the polymers had the same general MWD shape as the desired material, there was significant deviation between the anticipated and measured MWDs. It was proposed that these deviations were a result of termination of the living polymer chain ends and incomplete conversion of monomer, owing to experimental unfeasibility of excluding all impurities from the reaction setup.

In a separate semibatch process, monomer purity was taken into account to improve the fits[40]. In this work, the automatic control process accounts for the concentration of impurities in the reactor feeds. This model leads to better agreement between the predicted and measured MWDs[39] compared with the same system that did not take purity into account; however, there remained substantial deviations between these MWDs and the a priori desired distribution function (FIG. 1a). Although the presence of impurities was considered in the control model, termination of the active polymer chains can only be approximated. The discrepancies between the desired, predicted and measured MWDs are likely a consequence of the high sensitivity of the polymerization kinetics to the impurity concentration, which makes it difficult to accurately determine the initial concentration of alkyllithium initiating species. More recently, a fully automated control system was developed for continuous stirred-tank reactors using an inverse process model to gain better control of MWD shape in homopolymers[41]. This model assumes that each living polymerization leads to a uniform MWD (that is, each polymer in the sample has the same molar mass). Plotting the concentration of individual chains as a function of their chain length provides insight into polymerization behaviour in an isothermal batch reactor. This work was supported by previous studies that gave accurate predictions of MWD based on simplified polymerization kinetics, in which termination is not considered[42].

Box 1 | **MWDs and the limits of dispersity**

Polymer molecular-weight distributions (MWDs) are defined most typically using a combination of the molar mass averages, M_n and M_w, which are determined by size-exclusion chromatography and are defined as:

$$M_n = \frac{\sum M_i N_i}{\sum N_i}$$

$$M_w = \frac{\sum M_i^2 N_i}{\sum M_i N_i}$$

Using these two molar mass averages, $Đ$ is defined as:

$$Đ = \frac{M_w}{M_n}$$

which is related to the standard deviation (σ) of the distribution function by the relationship:

$$Đ = \frac{\sigma^2}{M_n^2} + 1$$

These equations reveal that $Đ$ is the relative breadth of the MWD function or, more specifically, it describes the standard deviation of chain lengths normalized to the number-average molar mass. Thus, $Đ$ provides information about MWD breadth only when the average molar mass of the polymers being compared is constant; that is, polymers can have the same $Đ$ but contain vastly different breadths of their respective MWDs[13,46,47,124].

In addition to being a limited description of the relative span of molecular weights in a polymer sample, $Đ$ offers no information on the shape of a distribution function. Fundamentally, a polymer's MWD shape can be varied infinitely while maintaining the same M_n and $Đ$. In fact, several reports have suggested that the absolute composition of polymer chain lengths should have a significant influence over polymer properties[20,63]. In recent years, the use of MWD shape for controlling polymer function without altering the chemical composition of the final material has become promising[45,48,75,77,100]. In this regard, looking towards the 'higher moments' or precise shape of the distribution becomes necessary (see BOX 2).

Box 2 | **MWDs and moments in probability statistics**

The majority of synthetic polymers contain a distribution of chain lengths. The corresponding molecular-weight distribution (MWD) functions are dependent on the kinetics of the polymerization reaction in question and have been described using a variety of probability functions. For example, the Flory–Schulz distribution is a single-parameter function that is typically used to describe the MWDs of polycondensation reactions[125]. This probability distribution is useful for modelling step-growth polymerization, which favours small chains, affording MWDs tailing towards high molar mass. For anionic polymerization processes, in which initiation is much faster than propagation, and termination reactions are nonexistent, the distribution of chain lengths is narrow and is accurately portrayed by the Poisson distribution[126]. Additionally, the shapes of distributions afforded through controlled radical polymerizations (such as atom-transfer radical polymerization) can be defined by the Schulz–Zimm distribution (a two-parameter function), because the initiation kinetics and termination events lead to a buildup of low-molar-mass polymer chains[18,63]. Furthermore, Gaussian or logarithmic normal distributions have been used to describe functions that are symmetric about the number-average molar mass[127].

A convenient parameter to describe the asymmetry of a MWD is the asymmetry factor (A_s), which gives a qualitative measure of the skew of a distribution. This factor is determined as the ratio of the distance from the peak maximum to the front of the peak over the distance from the peak maximum to the back of the peak at 10% of the peak height[128–131]. To avoid the difficulty of using a diverse array of functional forms to represent experimental MWDs, the concept of moments in probability statistics can be applied. The *n*th moment (μ_n) provides a specific quantitative measure of the shape of a distribution function and is described by $\mu_n = \int_{-\infty}^{\infty} (x - c)^n f(x)dx$ (REF. [128]). These mathematical descriptors are typically referred to as moments about some arbitrary value *c*. When $c = 0$, the moment is defined as raw or crude. The first raw moment is the expected value of *x* and, therefore, represents the mean or number average (μ) of the distribution. The second moment is often written as a central moment about the mean (where $c = \mu$) and corresponds to the variance of the distribution. Moreover, higher moments are most useful when reported in standardized form, which is found by normalizing the higher central moment (μ_n) to the previous moment (μ_{n-1}), so that comparison can be made between differently shaped distributions[130]. The third standardized moment is the skewness of the distribution and the fourth standardized moment describes its kurtosis.

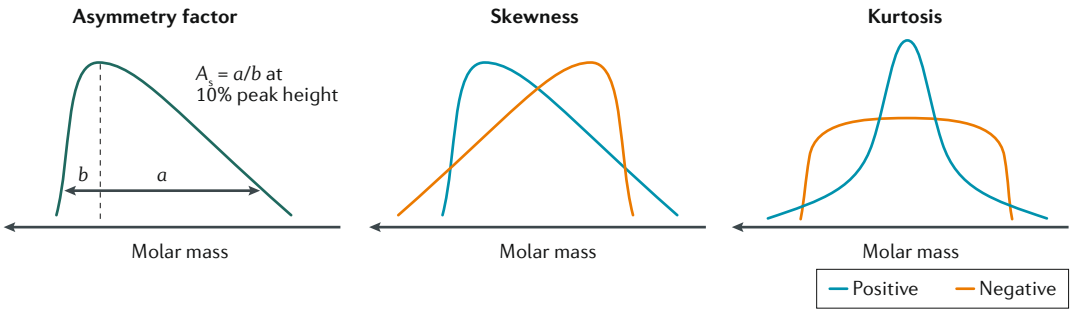

In addition to the processes described above, several studies have explored this phenomenon in a small-scale chemical laboratory setting. For example, Aoshima and colleagues developed a strategy for tuning the MWD function in diblock copolymers prepared through cationic polymerization (FIG. 1b), in which a solution of growing polymer chains was steadily added to a solution of a deactivating agent (aqueous ammonia) using a syringe pump to precisely control the addition rate[43]. This polymerization approach was suitable for tuning the MWD in a variety of vinyl ethers. A drawback of this process is that, to tune the MWD, the polymerization must be carried out in a syringe, which may not be suitable for polymerization reactions that require vigorous stirring[44]. In addition to the limited mechanistic scope of this method, controlled termination necessitates tuning of the block copolymer as the last step of the synthesis. This results in the loss of valuable information about the precise distribution function of the final polymer, because the MWD of each block cannot be decoupled from the overall measured MWD[14].

In addition to these controlled reactant feeds and termination methods for dictating polymer MWD shape, we developed a process for temporally controlled initiation in polymerization reactions that utilize a discrete initiating species[45]. Taking advantage of the kinetics of controlled polymerization processes, in which initiation is fast and all chains propagate at about the same rate, metered addition of a discrete initiating species dictates the molar quantities of each chain length. Initial proof of concept focused on nitroxide-mediated polymerization (NMP), whereby metering in a solution of alkoxyamine initiator at predetermined rates of addition afforded predictable control of polymer MWDs[45]. More specifically, polymers that are initiated early in the reaction afford chains with higher molar mass than those initiated later in the polymerization; therefore, the addition time of each initiating species dictates the length of that chain. Initially, constant rates of addition were used and longer addition times led to increased $Đ$. Furthermore, when the addition-rate profiles were altered from constant to linearly increasing rates, the polymers produced had distributions tilted into the low-molecular-weight region (asymmetry factor (A_s) < 1), corresponding to more polymers being generated later in the reaction. This study also revealed that using different initiator-addition-rate profiles was sufficient to yield polymers with the same M_n and $Đ$, but with different

MWD shapes. In all addition-rate profiles examined, $Đ$ and σ (standard deviation) were linearly related to the initiator-addition time, providing a convenient calibration curve for tuning the M_n, breadth and shape of the MWD. Moreover, this process offered the ability to prepare multimodal distributions as well as the synthesis of block copolymers with relatively low molar mass. This strategy was used to prepare a variety of well-defined block copolymers and could be applied to ATRP to show the utility of this process in manipulating MWDs in any controlled polymerization reaction that uses a discrete initiator[45]. In this case, the termination and initiation events inherent to the ATRP process were also shown to influence the MWD shape.

Although this approach provided command over the MWD shape, there are several issues inherent to NMP that render this process impractical for fundamental studies of the influence of MWD shape on polymer properties. For example, radical polymerizations have limited chain-end fidelity and cannot be run to full monomer conversion, which limits the practicality of this approach[46]. To address these challenges, the process of temporally controlled polymer initiation was extended to anionic polymerization processes, owing to their 'living' nature, broad monomer scope and ease of computational modelling to prepare functional block copolymers[47]. Therefore, we explored anionic polymerization of styrene in hydrocarbon solvents[48] (FIG. 1c). First, by adding alkyllithium initiating species at constant rates of addition, polymer MWDs were prepared with significant tailing into the low-molecular-weight region ($A_s > 1$). Conversely, exponentially increasing rate profiles were used to prepare polymers skewed substantially in the opposite direction ($A_s < 1$). The initiator-addition profiles for anionic polymerization were different to those in radical polymerization to achieve the same general shape of the polymer MWD, which is likely a consequence of the unique polymerization kinetics of each system: the anionic polymerization of polystyrene (PS) involves an equilibrium between a dormant lithium dimer aggregate and an active monomer species, whereas the kinetics of the aforementioned radical polymerization includes termination events.

In addition to using the conventional, thermally induced polymerization, photo-mediated strategies have been used to synthesize polymers with well-defined structures and architectures, owing to the broad utility of light as a stimulus. For example, photoinduced electron transfer-reversible addition fragmentation (PET-RAFT) polymerization in a flow reactor was introduced by Boyer and colleagues as an approach for governing polymer MWD composition[49,50] (FIG. 2a). Hypothetically, modification of the reaction rate or chemical concentrations during continuous flow would yield materials with different molecular weights that are then merged in the flow reactor to yield tailored MWDs. In this approach, the flow rates dictate the instantaneous concentration of reactive species, while the visible-light stimulus commands the overall reaction rate. Interestingly, by adjusting the irradiation intensity or wavelength at fixed flow rates, the monomer conversion could be controlled at each step of the process, dictating the precise mixtures of molar masses that are combined in the collection reservoir. Additionally, altering the flow rate or chemical concentration of the reagents under constant irradiation conditions afforded the same results. An advantage of the photoinduced continuous-flow process is the ability to prepare block copolymers with controlled compositional gradients of the blocks in their MWDs — a feature not yet achievable in conventional batch polymerization chain-extension processes. By altering the flow-reactor setup to separate each polymer fraction with a distinct molar mass in a plug-flow process, subsequent treatment of these fractions with a second monomer before entering a second flow reactor allows for the growth of a second block. This semicontinuous flow process allows each polymer fraction to be extended with a different quantity of the second monomer, thereby producing block copolymers with gradient compositions of molar

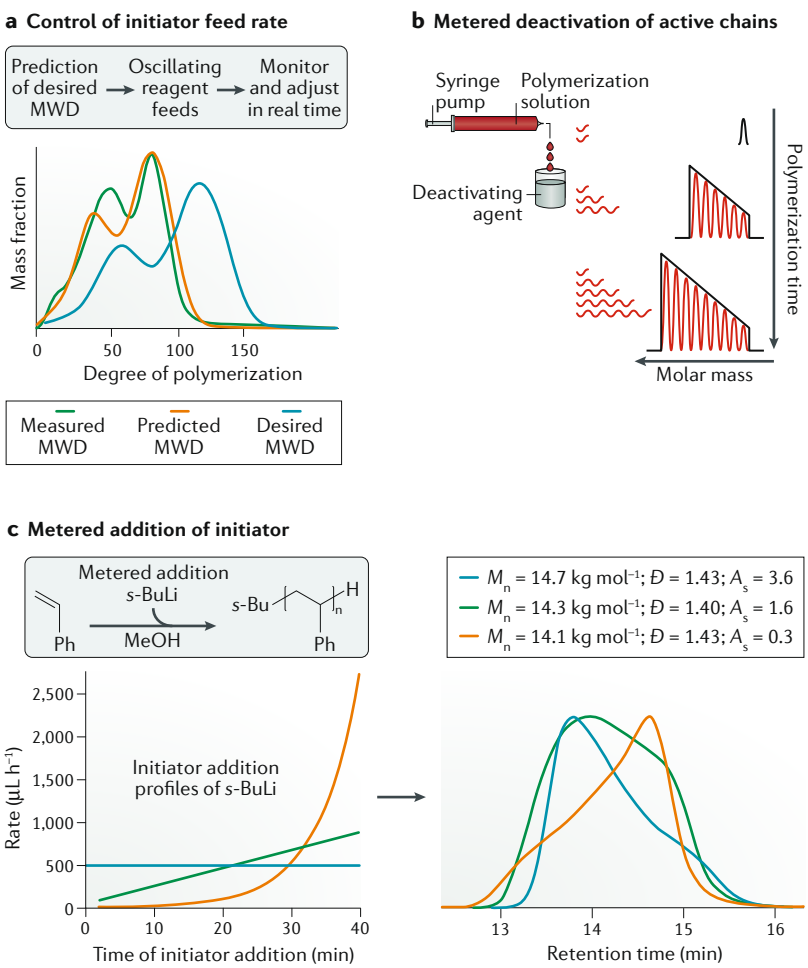

Fig. 1 | **Reagent and polymer feed strategies for temporal control of polymer MWD shape. a** | The desired, predicted and measured molecular-weight distributions (MWDs) from manipulating the monomer and initiator feed rates to a semibatch anionic polymerization. **b** | Strategy for manipulating polymer MWDs through the metered deactivation of active chains in cationic polymerization. **c** | Synthetic control of polystyrene MWD breadth and shape by metered addition of alkyllithium initiating species *sec*-butyllithium (s-BuLi) in anionic polymerization, showing three polymers with the same number-average molecular mass (M_n) and dispersity ($Đ$) but with very different MWD asymmetries. A_s, asymmetry factor. Panel **a** is adapted with permission from REF.[39], Wiley-VCH. Panel **b** is adapted with permission from REF.[43], Wiley-VCH. Panel **c** is adapted with permission from REF.[48], ACS.

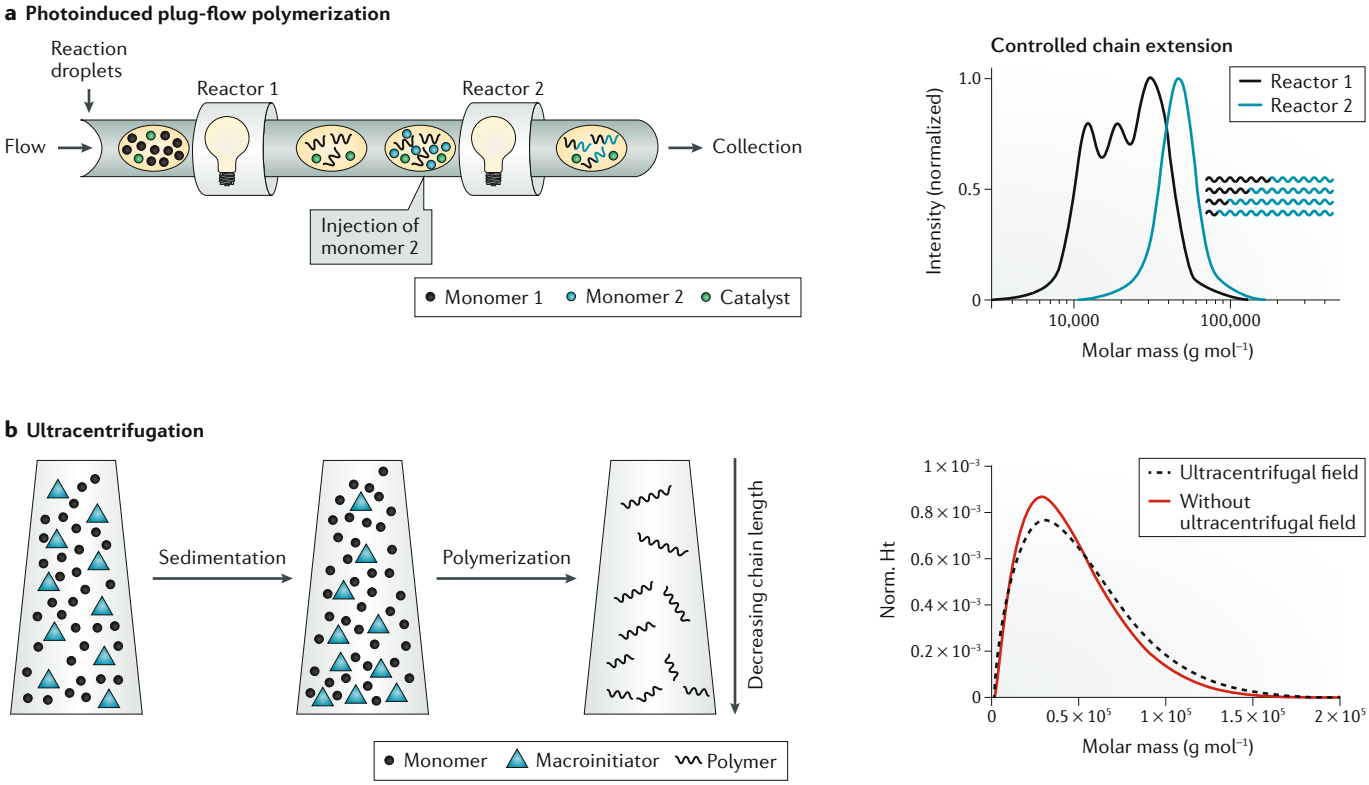

Fig. 2 | **Alternative methods for control of polymer MWD shape with photochemical or centrifugal stimuli.** **a** | Modified, photoinduced plug-flow polymerization reactor setup, which enabled the synthesis of block copolymers with compositional gradients. **b** | Illustration of molecular-weight distribution control through the use of ultracentrifugation to produce initiator-concentration gradients followed by polymerization. Panel **a** is adapted with permission from REF.[50], ACS. Panel **b** is adapted with permission from REF.[51], Wiley-VCH.

masses in both blocks in a single pass through the flow reactor (FIG. 2a). Although the level of control over MWD shape in this study was modest, likely because of unfavourable fluid-mixing behaviour, this work highlights an exciting opportunity for the use of photochemistry to fine-tune polymer MWDs.

In contrast with the previously mentioned processes that use reagent feeds or alterations of the polymerization reaction kinetics, Spinnrock and Cölfen developed a process for manipulating polymer MWDs using analytical ultracentrifugation[51] (FIG. 2b). Specifically, they exploited the well-established sedimentation equilibrium of chemical compounds in centrifugal fields to produce a desired concentration gradient of a macroinitiating species. With the monomer homogeneously distributed, photoinduced polymerization is then carried out in the centrifuge tube. The top and bottom of the reactor have lower and higher initiator-to-monomer ratios, respectively. By adjusting the centrifugal field, the precise concentration distribution can be fine-tuned, leading to good control of the final MWD. An advantage of this strategy is that the thermodynamics of analytical ultracentrifugation are well understood, which leads to good agreement between experimental and simulated MWDs. Although tuning the MWD through this approach is limited because it requires a macroinitiator for sedimentation to occur, this strategy could be extended to other types of chemical-concentration distributions through diffusion or mixing to give it greater practicality.

Block copolymer self-assembly

Although the influence of the breadth of polymer MWD (specifically, $Đ$) on the microphase separation of block copolymers has been widely studied[52–62], the effects of MWD shape (skew and kurtosis; BOX 2) remain largely unexplored. However, owing to the synthetic work outlined in the previous section, the community is beginning to investigate the importance of controlling the composition of MWDs. In this section, we explore the theoretical and experimental advances in understanding how changing the shape of an MWD affects the self-assembly of block copolymers.

Theoretical work in this area began with Leibler's transformative study that highlighted the potential significance of MWD composition on the phase behaviour of block copolymers[20,63]. Arbitrary A–B diblock copolymers with Schulz–Zimm distributions (SZDs) were compared with the equilibrium polymerization distributions (EPDs) at the same values of $Đ$. It is important to note that the SZD is often used to describe MWDs because it accurately portrays a large number of materials made by various addition polymerizations spanning $Đ = 1–2$ (REFS[18,19]). By contrast, the EPD specifically models the MWDs obtained from the equilibrium polymerization of lactide[63]. These two distributions diverge as the MWD

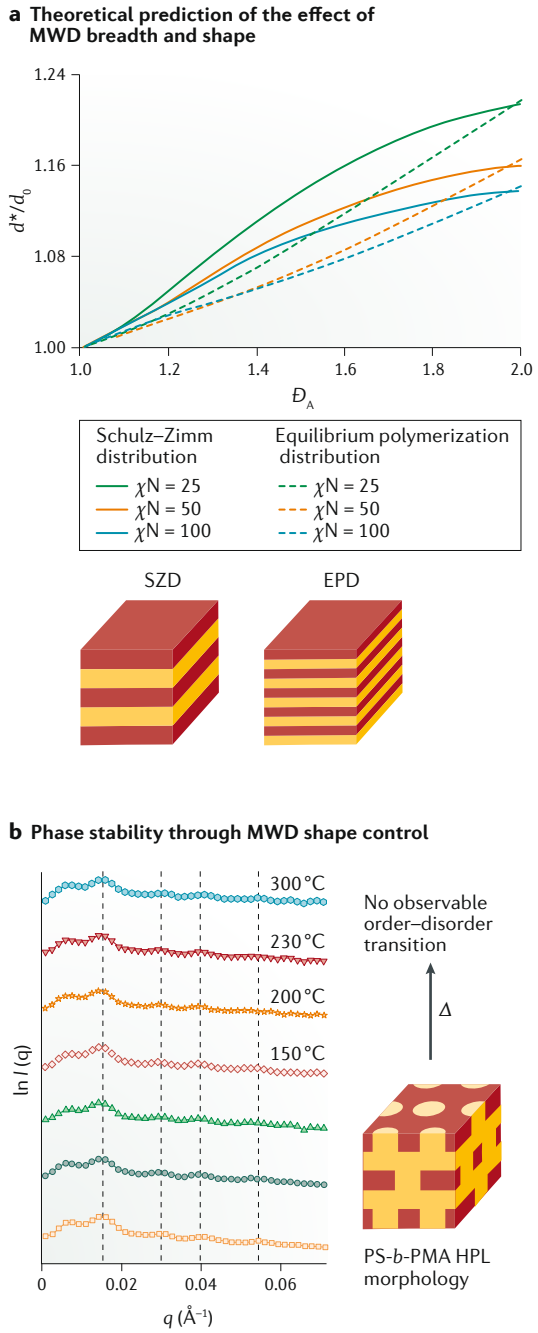

Fig. 3 | **Early work demonstrating the influence of MWD shape on the phase behaviour of block copolymers.** **a** | Predicted differences in the domain spacing (d^*/d_0) between the Schulz–Zimm distributions (SZDs, dashed lines) and the equilibrium polymerization distributions (EPDs, solid lines) in arbitrary A–B diblock copolymers, where the A-block molecular-weight distribution (MWD) breadth ($Đ_A$) and shape are modified with a constant volume fraction of 0.5. Data are shown for three different segregation strengths (χN). **b** | Small-angle X-ray scattering measurements of polystyrene-*block*-poly(methyl acrylate) (PS-*b*-PMA) with a broad and symmetric PS block, showing unprecedented stability of the perforated lamellar phase (P). The dotted lines are indexed to the P phase. HPL, hexagonally perforated layer; *I*, intensity; *q*, the scattering vector. Panel **a** is adapted with permission from REF.[63], ACS. Panel **b** is adapted with permission from REF.[33], ACS.

span increases, reaching their maximum difference at $Đ = 1.5$, and converge to similar shapes as $Đ$ approaches 2. The domain spacing (d^*), an important parameter in determining the properties of block copolymers such as those found in lithographic and photonic materials, predicted by self-consistent field theory (SCFT) of the aforementioned A–B diblock copolymers, was then compared with that of their monodisperse counterparts (d_0)[63] (FIG. 3a). In these studies, only the MWD of the A-block in the A–B diblock copolymer was altered, while the B-block remained narrow. The domain spacing of the materials increased with increasing $Đ$. However, there was a striking difference in d^*/d_0 between the two MWD shapes, with the largest disparities at $Đ \approx 1.5$, at which the compositions of chain lengths diverge most sharply.

The differences observed between the SZD and the EPD in the aforementioned study can be explained as follows. First, the SZD and the EPD have different entropic elasticities; that is, the presence of a broad distribution decreases the entropic penalty for stretching a domain because the long chains can more easily fill the empty space[30,55,62,64,65]. In this regard, the EPD has a larger relative quantity of long-chain polymers and, thus, its increased d^*/d_0 with respect to the SZD are in good agreement with theory. Second, domain spacing can increase by having small polymers desorb from the interface and swell the phase of their majority component. This effect is a balance of the gain in entropy by having a short A-block in the B-phase with the loss in enthalpy from surrounding an A-block with dissimilar B-segments. This effect is more pronounced at lower values of the Flory interaction parameter, in which the A-block and B-block are more miscible, leading to larger A-segments being pulled into the B-phase[27,30,64,66,67]. At $Đ \approx 1.5$, the EPD also has a much larger population of very short polymer chains. Both domain-spacing-enhancement mechanisms are in accordance with theoretical predictions. In addition to the differences in domain spacing between the SZD and the EPD, the influence of these distribution shapes was also examined on the phase diagram of arbitrary A–B diblock copolymers[68]. Interestingly, compared with the relatively large deviations in domain spacing between the two MWDs, only small differences in the phase diagram were predicted by SCFT. For example, when the modified A-block is in the minority phase, the EPD has cylinder and lamellar phase boundaries that are slightly shifted to lower volume fractions. It was hypothesized that, although the decreased entropic stretching penalty induced curvature towards the disperse A-block, this impact can be effectively offset by swelling of the B-domain through chain pull-out of the A-phase, which pushes the phase boundary in the opposite direction. It is through these two proposed mechanisms that the influence of MWDs on block copolymer phase behaviour can be described.

In contrast with simulations (as discussed in the aforementioned study), which suggest that MWD shape has only minor effects on the compositional phase diagram of block copolymers, experimental work by Matyjaszewski and colleagues has revealed that the skew of the distribution function has a marked impact on

self-assembly. Specifically, they explored the effects of distribution asymmetry on the formation of metastable morphologies, such as hexagonally perforated layers, in diblock copolymers of poly(styrene-*b*-methyl acrylate)[33]. In this work, adjusting the amount of the catalyst was used to manipulate the reaction kinetics, leading to a broadening of polymer dispersity. The dispersity-controlled polymers can then be chain-extended with another monomer to afford well-defined block copolymers with one narrow block and one broad block. Although this process does not offer the ability to govern the precise MWD shape, it does yield polymers with more symmetrical distribution functions than most synthetically accessible polymers, which follow the positively skewed SZD[32]. This synthetic process therefore affords an interesting way to examine the effects of skew on the self-assembly of block copolymers.

Morphological differences have been observed between two polystyrene-*block*-poly(methyl acrylate) (PS-*b*-PMA) copolymers with similar block composition and overall molar masses, in which the PS block was either narrow or broad and symmetric[69]. Specifically, small-angle X-ray scattering (SAXS) studies revealed that the polymer with a narrow PS block exhibited a morphology of hexagonally packed cylinders (C), whereas its counterpart with a broad and symmetric PS block displayed hexagonally perforated layers (P), which is traditionally understood as a metastable morphology. The stability of the P phase block copolymer was then examined in a variety of ways. First, the same sample was subjected to a library of different solvent-casting and thermal-annealing conditions. Intriguingly, no change in the overall morphology was observed for any of the different sample preparations. In a different experiment, the overall thermal stability of the P phase was examined by temperature-dependent SAXS experiments[33] (FIG. 3b), in which the sample was repeatedly heated to higher temperatures before X-ray data collection. Even up to 300 °C, no order–order or order–disorder transitions were observed. Although these experiments do not provide definitive proof that this P phase is the equilibrium morphology, they do provide strong evidence for the enhanced stability of the P phase in PS-*b*-PMA with broad and symmetric PS MWDs. This study is particularly noteworthy given other examples in the literature that show clearly that the P morphology is metastable and, therefore, difficult to access, in both narrow and broadly dispersed block copolymers[70–72].

The mean interfacial curvature of the P phase has a large standard deviation[73,74]. These large differences in curvature between local environments result in chain packing frustration, which typically renders the P phase (as well as other phases, such as the double diamond) stable only in a relatively narrow temperature range or close to the order–disorder transition. It was hypothesized that the broad and symmetric distributions compensate for large disparities in mean curvature between local environments[33]. Thus, equal portions of large and small polymer chains in the broad distribution may alleviate chain packing frustration more favourably than skewed distribution functions, such as the SZD. Although additional theoretical and experimental investigations are needed, this study demonstrates the importance of considering the entire distribution of molar masses in a polymer sample when determining phase behaviour[33].

In more recent work towards controlling the MWD shape in block copolymers, we prepared three sets of polystyrene-*block*-poly(methyl methacrylate) (PS-*b*-PMMA) copolymers: one with narrow MWDs of both blocks as a control group; a set with a positively skewed PS block but narrow PMMA block; and a set with negatively skewed PS blocks but narrow PMMA blocks[75]. The molar mass and breadth of the PS blocks were held constant to study only the influence of MWD skew, and the amount of PMMA in each block was increased to explore a range of overall molecular weights. The self-assembly behaviour was then examined by grazing-incidence SAXS measurements. All polymers examined in this study exhibited lamellar morphologies but showed large differences in domain spacing. As expected, the narrow control group with two narrow MWDs showed increases in d^* with overall molar mass, in accordance with the generally understood relationship outlined by Matsushita and Papadakis[22,76] (FIG. 4a, top panel (green)). However, when the dispersity was broadened and the PS MWDs were skewed to give a high molar mass tail, substantial increases in d^* were observed relative to the narrow MWD counterparts (FIG. 4a, top panel (orange)). More interestingly, when the dispersity was broadened and the MWD skewed to give a low molar mass tail, even greater increases in d^* were revealed (FIG. 4a, top panel (blue)). The data revealed that both the $Đ$ and the MWD skew are important parameters to consider when determining the lamellar period of block copolymer thin films.

It is hypothesized that the large increases in domain spacing observed in this study are due to small PS chains withdrawing from the interface and swelling the PMMA phase (that is, the chain pull-out mechanism outlined by Matsen and others)[64–67]. This hypothesis is supported by the fact that increasing the fraction of PMMA in the overall diblock copolymer increases the deviation in d^* between different MWD shapes. In this swelling mechanism, larger PMMA blocks enable larger PS segments to desorb from the interface; thus, a higher quantity of PS pulled into the PMMA phase would result in larger enhancements in domain spacing. In addition to this observation, the positively skewed PS-*b*-PMMA samples ($A_s > 1$) result in a larger divergence of d^*, presumably because they have a larger percentage of very low molar mass PS chains. We used population statistics and least-squares analysis to construct a statistical model for predicting d^* based on overall molar mass, MWD breadth and MWD skew[75]. This theoretical investigation not only provided a simple process for predicting d^* of block copolymers with high fidelity but also elucidated fundamental relationships between MWD shape and the lamellar period of block copolymer thin films. We discovered that MWD skew influences the domain spacing on the same order of magnitude as the breadth of the MWD, demonstrating that the skew is just as important as $Đ$ in determining polymer properties, as seen in FIG. 4a (lower panel). Plotting the cumulative contributions from the statistical model reveals that

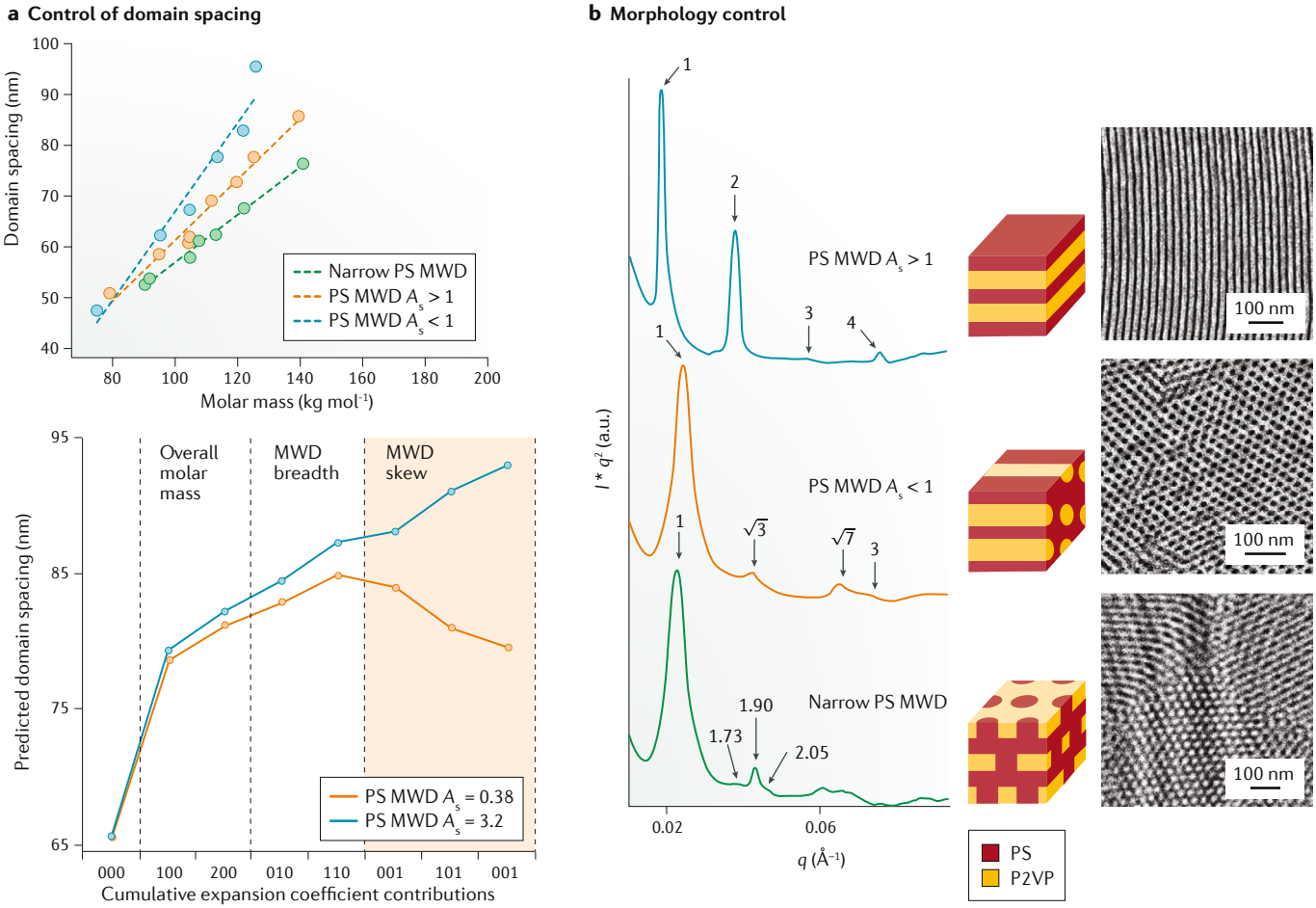

Fig. 4 | **Studies demonstrating the influence of MWD shape on the phase behaviour of block copolymers.** **a** | Relationship between domain spacing (d^*) and the overall molar mass, polystyrene (PS) molecular-weight distribution (MWD) breadth and PS MWD skew of lamellar thin films of polystyrene-*block*-poly(methyl methacrylate) (PS-*b*-PMMA; top). Predicted domain spacing of two polymers with the same M_n, volume fraction and $Đ$, showing large deviations based on the skew of the PS block (bottom). **b** | Polystyrene-*block*-poly(2-vinylpyridine) (PS-*b*-P2VP) samples with the same M_n and PS volume fraction display three distinct morphologies based on the shape of the PS MWD. A_s, asymmetry factor; $Đ$, dispersity; I, intensity; M_n, number-average molar mass; q, the scattering vector. Panel **a** is adapted with permission from REF.[75], ACS. Panel **b** is adapted with permission from REF.[77], ACS.

incorporation of M_n and $Đ$ into the statistical model results in essentially no change in the predicted d^*. However, when the skew components of the PS MWD are integrated into the model, substantial deviations arise in lamellar periods, accounting for the experimentally observed differences.

In addition to the influence of MWD shape on the d^* of block copolymer thin films, we also explored the impact of MWD shape on the bulk phase diagram for diblock copolymers, in which one block had a modified MWD shape[77]. We prepared polystyrene-*block*-poly(2-vinylpyridine) (PS-*b*-P2VP) samples in an analogous fashion to those produced in the aforementioned study of PS-*b*-PMMA thin films[78]. Three sets of samples were prepared with constant M_n of the PS block but with narrow MWD, broad with positively skewed MWD and broad with negatively skewed MWD. Each sample was chain-extended with different amounts of P2VP to investigate a broad range of the phase diagram. Interestingly, no statistically significant differences in d^* were observed for polymers exhibiting the same overall morphology, supporting our hypothesis that the chain pull-out mechanism of domain-spacing enhancement is not at play.

Although no differences were in observed in d^*, SAXS measurements revealed substantial variation in the overall morphology, depending on the shape of the PS MWD. Specifically, in a sample with a low volume fraction of the PS block, the phase boundary between the lamellar (L) phase and the C phase was pushed significantly towards higher volume fraction for both broader-$Đ$ polymer classes (skewed to high and low molecular weights). Additionally, by manipulating the skew of the PS block, the distance that the L/C phase boundary moved could be fine-tuned. Positively skewed samples pushed the L/C boundary towards lower PS volume fraction, whereas negatively skewed PS blocks induced the L/C boundary to move towards higher PS volume fraction compared with samples with narrow MWDs. This divergence in phase behaviour is exemplified by the

observation of three distinct morphologies in a polymer with the same M_n and volume fraction[77] (FIG. 4b). In this instance, the polymer with narrow PS MWD displayed the perforated layer morphology (P phase), whereas the positively and negatively skewed samples showed L and C phases, respectively.

These findings provide strong support for the idea that the preferred interfacial curvature of a self-assembled block copolymer is not merely reliant on the span of molar masses in a sample but on the precise mixture of chain lengths — an observation that is in agreement with the hypothesis of Matyjaszewski and colleagues[33]. The materials skewed to low molar mass agree well with previous reports, in which it was posited that broad distributions fill empty space more efficiently by possessing decreased entropic stretching penalties, thereby inducing curvature towards the disperse block. By contrast, samples skewed to higher molar mass do not follow this trend and curvature away from the disperse block was observed. This influence can be explained qualitatively through the different relative quantities of long and short PS chains. The samples skewed to high molar mass have a large portion of high molar mass PS blocks, which can more effectively extend to fill empty space as the curvature towards the disperse block is increased. By contrast, materials with PS blocks skewed to low molecular weight have a substantial fraction of extremely low-molecular-weight material. These small chains prefer not to stretch to fill empty space, instead remaining relaxed at the interface, which reduces the propensity for the disperse block to be on the inside of interfacial curvature. The results in this section demonstrate the promising utility of MWD shape as a means to tailor block copolymer phase behaviour, providing the opportunity to manipulate polymer properties in a one-reactor setup. As observed, MWD shape has a profound influence on d^* and the phase diagrams for block polymers, opening the door to using MWD shape to tailor all aspects of block copolymers without altering their chemical composition. Theoretically, this enables tuning of a material's photonic properties, as well characteristics such as toughness, strength and elasticity.

Rheological and mechanical properties

The effects of M_n, M_w and $Đ$ on physical properties such as tensile strength, toughness and viscosity have been studied since the 1960s. Although early studies suggested that the influence of MWD shape should influence such rheological and mechanical properties, little work has been done to systematically understand how they are affected by skew. Many of the first theories used to predict rheological behaviour assumed a monodisperse system[78–83]. However, early experimental evidence indicated that these theories break down with variations in MWD shapes. For example, Middleman's early work on rheological properties led to one of the first observations that "undoubtedly, no single average of molecular weight will be sufficient to allow a unique reduced variable correlation to describe precisely the viscosity curves of a wide class of materials, in view of the fact that the curves are sensitive to the shape of the MWD, for which [$Đ$] is not a unique measure"[90].

The characterization of polymers through rheological and mechanical measurements is routinely preformed in the polymer industry to understand the processability of the materials in the melt state. Viscosity is the most important parameter for describing the flow of a polymer. Because polymers are non-Newtonian fluids, they often exhibit shear thinning behaviour, which means that, at higher frequencies, longer polymer chains begin to orient themselves along the direction of the applied stress (flow). $Đ$ and skew of the distribution would reasonably be expected to have a significant effect on flow behaviour because of the dependence of viscosity on chain entanglements. Based on this hypothesis, there have been many attempts to correlate MWD to the melt flow index (MFI), which is typically reported as the mass of polymer that flows out of a capillary in 10 min with a given applied force (inversely proportional to viscosity). Using the power law relating zero shear viscosity (η_0) to M_w as a basis for mathematical models ($\eta_0 \propto M_w^{3.4}$), many theories have been developed to predict the MWD and MWD shape based on the MFI. For example, some work has shown a correlation of 1/MFI with $(M_w)^x$ (x = 3.4–3.7) for linear polymers, whereas branched polymers tended to best correlate with –ln(MFI) and M_v (the viscosity-average molecular weight)[84]. Although this work accurately predicted trends observed with linear homopolymers, it lacked the ability to precisely model branched polymers or polymer blends. More recently, Pérez-Chantaco and colleagues were able to fit a single equation to predict MWD breadths of both linear and branched polyethylenes with $Đ$ ranging from 2 to 20; however, this model is designed particularly for polyethylenes and would require a different set of modelling equations to account for branching and dispersity of other polymers[85].

The storage modulus (G') and loss modulus (G'') of a polymer blend are also of importance for understanding its mechanical properties. The crossover point (when $G' = G''$) occurs at a frequency that corresponds to the shift from viscous to elastic behaviour, and has been used as a surrogate for describing the MWD of a polymer[86]. Polymers with a greater weight fraction of high-molecular-weight chains (that is, a large M_w) typically have a crossover point at lower frequencies than polymers with lower-molecular-weight chains. Similarly, samples of narrow $Đ$ have been shown to hold a crossover point at higher moduli values than samples with broader $Đ$[87]. MWD effects on the rheology of high-density polyethylene samples made from Ziegler–Natta and metallocene-derived catalysts have also been studied and support this inverse correlation between the crossover modulus (G_c) and $Đ$[88]. More importantly, it was shown that higher moments of the MWD, such as the z-average molecular weight, as defined by Eq. 1, give better correlation with the crossover modulus[88]. Plotting M_z/M_w as a function of G_c exhibited a much greater linear fit than $Đ$ as a function of G_c, thus emphasizing that $Đ$ alone is not a true measure of polymer properties[88].

$$M_z = \frac{\sum M_i^3 N_i}{\sum M_i^2 N_i} \quad (1)$$

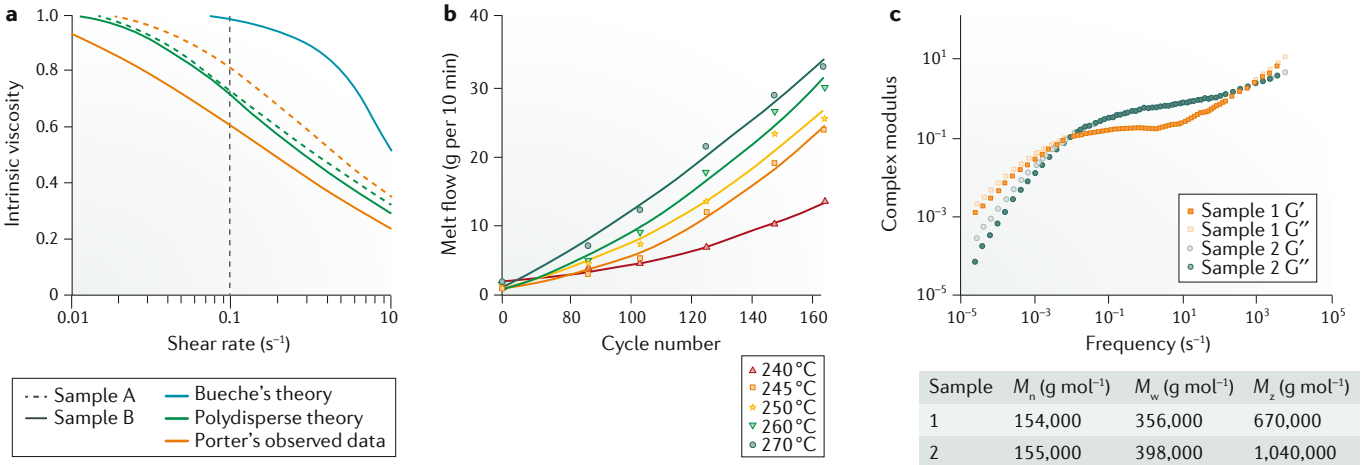

Sample	M_n (g mol^{-1})	M_w (g mol^{-1})	M_z (g mol^{-1})
1	154,000	356,000	670,000
2	155,000	398,000	1,040,000

Fig. 5 | **Early theoretical and experimental work showing the influence of *Đ* and MWD shape on the rheological properties of polymers. a** | Intrinsic viscosity as a function of shear rate data for two different solutions of polyisobutylene, where sample B is a more dilute solution than sample A. Experimental data observed by Porter is compared with Middleman's polydisperse theory and Bueche's original theory. By taking dispersity into account, Middleman's model fits more closely to the experimental data; however, it is still difficult to distinguish between the different isobutylene solutions. **b** | Melt flow index for polypropylene after *N* extrusion cycles at different temperatures. Because of the increased amount of chain scission at elevated temperatures, the melt flow index increases, corresponding to a decrease in viscosity. **c** | Comparison of the dynamic modulus master curve for polystyrene blends (sample 1 and sample 2), showing a large difference in complex modulus between the two samples at low frequencies due to the differences in *z*-average molar mass (M_z). M_n, number-average molar mass; M_w, weight-average molar mass; MWD, molecular-weight distribution. Panel **a** is adapted with permission from REF.[90], Wiley-VCH. Panel **b** is adapted with permission from REF.[97], Elsevier. Panel **c** is adapted with permission from REF.[98], copyright (1992), The Society of Rheology.

Others have also noted that changes in *Đ* influence rheological properties, showing that non-Newtonian behaviour often occurs at higher shear rates for polymers that are monodisperse than for polymers with broader dispersities[85,89,90]. For example, the relationship between *Đ* and viscoelastic behaviour of PS samples was investigated[89]. It was observed that disperse blends of PS fit the power law relationship between stress and shear rate better than monodisperse blends. By measuring the flow curves of each sample, it was apparent that melt viscosity of broad-*Đ* PS strongly correlates with M_w at low shear rates but correlates more strongly with M_n at higher shear rates. Furthermore, at low shear rates, PS melts with broader *Đ*, exhibit less temperature-sensitive melt viscosities than samples with narrow *Đ*[89]. To help expand theoretical models in accounting for variations in dispersity, Middleman adapted Bueche's theory[89]. By taking dispersity into consideration, Middleman devised a polydisperse model that led to a better fit with experimental viscosity data presented by Porter[90]. Although neither Bueche's nor Middleman's theoretical models exactly match the observed data, the trends are closer when taking *Đ* into account (FIG. 5a).

Mathematical theories were also developed to account for the effects of *Đ* and MWD on the rheological properties of polymer melts[91–94] For example, a superposition model was used to define the relationship between MWD and shear viscosity, exemplifying that high-molecular-weight fractions dominate viscoelastic behaviour at lower shear rates, whereas low-molecular-weight fractions dominate at higher shear rates[95]. This model makes it possible to accurately predict the rheological behaviour of blends of homogenous polymers with different MWDs, which is what many earlier models sought to accomplish.

The MWD has been used to enhance polymer properties in developing commercial products through the technique of polymer blending. For example, although not in continuous monomodal distributions, blending can be used to alter the MWD by influencing the shape and skew. Incorporation of a small amount of high-molecular-weight or low-molecular-weight chains into a polymer sample can cause considerable variations in processing and properties. Taking a narrow PS sample (M_n = 247,000 g mol^{-1}, *Đ* = 1.08) and blending in increasing amounts of low-molecular-weight PS (M_n = 78,500 g mol^{-1}, *Đ* = 1.08), Rudd showed a linear inverse correlation between zero shear viscosity and percent incorporation of low-molecular-weight PS[96]. Similarly, understanding polypropylene chain scission during polymer extrusion has shown that increasing the low-molecular-weight tail of the MWD can drastically affect the rheological properties[97]. At higher extrusion temperatures, chain scission of polypropylene occurs, thus increasing the weight fraction of low molecular polypropylene chains. With a skew towards low molecular weight, fewer entanglements in the polypropylene blend result in a decrease of viscosity, as shown by an increase of the melt flow index[97] (FIG. 5b).

The effects of blending on the rheological behaviour of narrow-*Đ* commercial PS samples were also explored. The dynamic modulus master curves of two blends were measured for narrow-*Đ* PS samples, in which each blend had roughly the same M_n and M_w but a vastly different M_z, which is especially sensitive to high-molecular-weight tailing of the MWD. A substantial,

a Control of Young's modulus

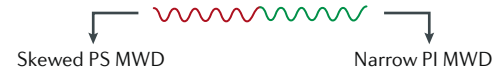

Entry	M_n (S) (kg mol^{-1})	$Đ$ (S)	A_s	M_n (SI) (kg mol^{-1})	$Đ$ (SI)	E (MPa)
1a	14.1	1.19	1.85	35.6	1.14	460
1b	14.2	1.22	0.52	35.1	1.16	560
2a	14.9	1.42	3.52	36.8	1.21	450
2b	14.1	1.39	0.37	33.6	1.22	530
3a	15.2	1.69	4.48	36.3	1.25	220
2b	14.1	1.71	0.31	36.5	1.28	440
3a	14.4	2.01	4.97	37.2	1.28	85
2b	13.8	1.97	0.26	34.4	1.29	300

b Control of viscosity

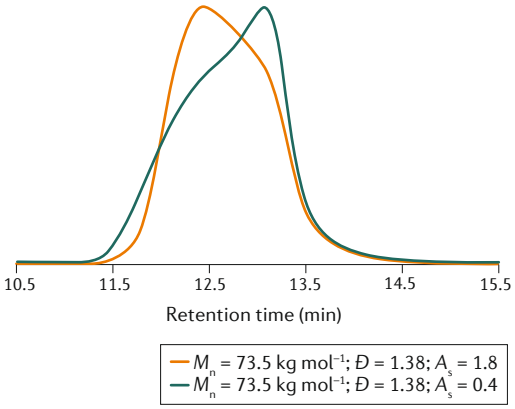

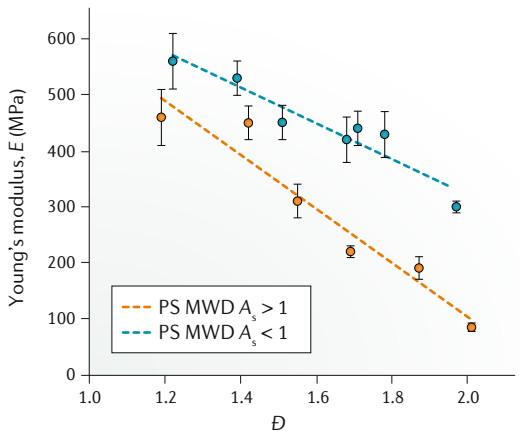

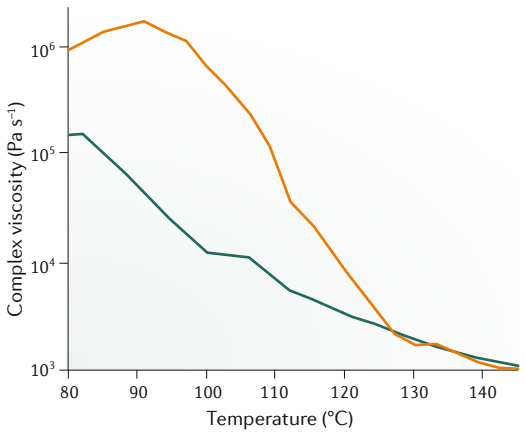

Fig. 6 | **Recent work showing the influence of MWD shape on the mechanical and rheological properties of homopolymers and block copolymers. a** | Poly(styrene-*block*-isoprene) (PS-*b*-PI) block copolymers with the same overall number-average molar mass (M_n) and Young's modulus (E) for each sample. The plot is of PS dispersity ($Đ$) as a function of E. Blue circles indicate samples with PS blocks that have asymmetry factor (A_s) < 1 and red circles indicate samples with PS A_s > 1. **b** | Gel permeation chromatography traces of two PS samples with the same M_n and $Đ$ but opposite skew. The plot shows complex viscosity profiles at various temperatures of the two PS samples. MWD, molecular-weight distribution. Panel **a** is adapted with permission from REF.[48], ACS. Panel **b** is adapted with permission from REF.[100], Wiley-VCH.

threefold difference in complex modulus between the two blends at low frequencies was observed (FIG. 5c). This indicated that the effects of a high-molecular-weight tail significantly influence the rheological behaviour of the sample[98]. Similarly, industrial production of plastics takes advantage of polymer blending to create materials that allow for easy processing, while also rendering the material commercially viable. For example, in industrial processing of polyethylene, blending is used because high-molecular-weight tailing helps improve material toughness, whereas low-molecular-weight chains lower viscosity and improve processing. Simply adding a few weight percent of ultrahigh-molecular-weight polyethylene allows for variations in the MWD shape that can increase the stiffness[99].

More recently, we explored the influence of MWD shape on the rheological and tensile properties of poly(styrene-*block*-isoprene) (PS-*b*-PI), in which the shape and $Đ$ of the PS block were varied using the aforementioned method of discrete initiation[48]. A library of PS-*b*-PI samples was made, in which the PS block was skewed to either high or low molecular weight with varying $Đ$. We observed that all samples with a PS block skewed to high molecular weight (A_s < 1) had consistently higher Young's modulus (E) values than the corresponding block copolymers with a PS block skewed to low molecular weight (A_s > 1). Furthermore, as $Đ$ increased and the difference between the A_s values of the corresponding block copolymers widened, the difference in E exceeded that of samples with PS skewed to higher molecular weights by a factor of 3.5 (FIG. 6a). This difference in E was a clear indication that MWD shape alone (without alteration of $Đ$ or M_n) has a significant influence over the polymer properties, giving promise for a systematic approach to fine-tuning polymer properties.

We further investigated the effect of MWD shape on rheological properties of PS samples with the same M_n and $Đ$[100] (FIG. 6b, top panel). We observed that the MWD with a low-molecular-weight tail held a higher glass transition temperature (T_g), an increased stiffness, increased thermal stability and a higher apparent

viscosity than the corresponding sample with a high-molecular-weight tail, which was attributed to variation of the chain-length composition. A greater number of lower-molecular-weight chains requires less thermal energy to disentangle and flow, thus decreasing the T_g. Furthermore, the rates of shear thinning were almost identical between the two samples (FIG. 6b, bottom panel), with the PS samples with MWD tailing towards low molar mass exhibiting up to threefold higher apparent viscosity than that of the PS with skewing towards high molar mass at 25 °C. Even above the T_g, at 150 °C, there was a substantial difference between the apparent viscosity of the two samples, with the sample tailing to high molecular weight still maintaining a twofold to threefold greater increase in the apparent viscosity than the sample tailing to low molecular weight. The observed rheological differences between the two samples can be explained through reptation theory, in which the PS sample which has a higher weight fraction of high-molar-mass chains, retains a greater number of entanglements, thus reducing the mobility of chains and increasing the viscosity.

Finally, we showed[100] that the degradation temperature could be increased by 10 °C, simply by selecting a sample with a certain MWD shape over that with the opposite shape. This degradation is presumably because a larger fraction of high-molecular-weight chains improves the thermal stability. By being able to tune the viscosity, T_g and thermal stability of polymers, optimal processing and property relationships can be achieved. For example, in hot-melt extrusion, very high shear rates and temperatures are used, and the optimal complex viscosity range is 1,000–10,000 Pa s^{-1}. Because the complex viscosity can be adjusted by changing the shape of the MWD, lower temperatures can be used to reach the same desired viscosity needed for polymer processing.

Outlook

To achieve the goal of manipulating a polymer's properties without adjusting its chemical composition, a number of methods have been developed to precisely tune the breadth and shape of polymer MWDs for different polymerization processes and monomer types. Reagent feeds and controlled initiation and termination processes enable the molar quantities of each chain size in a polymer sample to be precisely controlled[38–48]. Although precise control of the total MWD has been well developed for a limited set of polymerizations (specifically, NMP and anionic)[45,48,75,77], this remains to be achieved for all types of polymerization. In theory, discrete initiation can be implemented in any living polymerization system, including ring-opening metathesis and coordination–insertion polymerizations, allowing for the production of polyolefins with monomodal, skewed MWDs. Alternatively, ultracentrifugation and photocontrolled polymerization strategies can be applied for dictating the composition of polymer chain lengths in a given material[49–51]. The use of such synthetic strategies has validated earlier theoretical predictions and elucidated the profound influence of MWD shape over an array of polymer properties. For example, initial predictions suggested that block copolymer domain spacing should be impacted by the symmetry of the MWD[5]. Subsequent experimental studies confirmed that domain spacing, as well as the overall morphological phase diagram, can be predictably manipulated by altering the precise shape and symmetry of the MWD of the final material[33]. The MWD shape also has a significant influence over the rheological and mechanical properties of homopolymers and block copolymers[38,48,75,77]. Although an impact of MWD shape on these properties has been proposed for decades, only recently have scientists been able to empirically study these structure–property relationships.

The use of MWD shape to tailor polymer properties is still in its infancy, but many encouraging opportunities in photonic materials, thermoplastic elastomers, microelectronics, drug delivery and plastics await. This platform for fine-tuning the mechanical properties and processing parameters of commercial polymers without the need to alter the chemical identity of the desired material is promising from an economic perspective[101]. Moreover, the profound influence of MWD on the domain spacing of block copolymers is advantageous for the fabrication of photonic polymers with precisely defined absorption and reflectance windows for applications in energy-efficient windows, optical-fibre claddings and coatings for extended material lifetimes[74,102–106]. Additionally, an ability to dictate the phase boundaries of the morphological phase diagram of self-assembled block copolymers using MWDs is promising from the perspective of thermoplastic elastomer applications and materials with functions that depend greatly on the physical properties of the constituent monomers and the overall microstructure[48,107–113]. Command of the phase behaviour of block copolymers in this fashion may also enable bicontinuous structures for use in microfiltration[114–117]. Furthermore, modifying the MWD shape may offer utility to the field of drug delivery, as the composition of a polymer may provide control over the release of bioactive compounds[118,119]. Currently, synthesis of these materials has been limited to a laboratory scale. However, large-scale reactions for industrial application are not far from reach. Notably, BASF has already implemented a method for broadening PS samples through the use of controlled addition of monomer, initiator and rate-retarding agents[120].

More fundamental studies are needed to fully elucidate the relationship between MWD and polymer structure and function. The ability to extract examples from the literature to investigate the effects of MWD would be greatly beneficial to the realization of this approach and a cohesive theory of MWD shape. Thus, it would be highly advantageous for scientists and engineers to report asymmetry factors, skewness, kurtosis and/or even the higher moments of the distribution function in addition to their molar masses and dispersities. In addition, comparison of MWDs from different size-exclusion chromatography (SEC) instruments poses an additional problem because SEC typically provides relative molecular-weight information. In this regard, MWDs determined through multi-angle laser-light-scattering measurements may be more advantageous, as they afford absolute measurements on polymer

molecular weights and MWDs that can be accurately compared across multiple instruments[121]. Moreover, a particularly challenging aspect of this research is the efficient characterization and separation of polymers with distributions of chain lengths or composition in one or multiple blocks by SEC[122,123]. In this vein, additional effort is necessary to expand our analytical toolbox to more effectively characterize complex mixtures of macromolecules. Such efforts are necessary for accurate characterization of polymers in which the modified MWD is not in the first block or in which the homopolymer or block copolymer has multiple MWDs with systematically deviating shapes. Finally, although models exist to describe certain properties, such as domain spacing, we are still unable to predict how the MWD shape of a continuous distribution affects block copolymer macrophase separation — the development of such computational models remains a great challenge in polymer science. In general, accurate and precise models remain difficult because each polymerization mechanism follows different reaction kinetics, behaves differently in a variety of solvents and does not always account for impurities in a standard laboratory setup. Overall, we anticipate that varying polymer MWDs will enable chemists, materials scientists and engineers to prepare polymers with new and previously inaccessible combinations of properties, without the need to alter the chemical composition of the target material.

Published online: 01 October 2019

1. Bates, F. S. et al. Multiblock polymers: panacea or Pandora's box? *Science* **336**, 434–440 (2012).
2. Bates, F. S. et al. Block copolymer thermodynamics: theory and experiment. *Annu. Rev. Phys. Chem.* **41**, 525–557 (1990).
3. Nichetti, D. et al. Influence of molecular parameters on material processability in extrusion processes. *Polym. Eng. Sci.* **39**, 887–895 (1999).
4. Collis, N. W. et al. The melt processing of monodisperse and polydisperse polystyrene melts within a slit entry and exit flow. *J. Non-Newtonian Fluid Mech.* **128**, 29–41 (2005).
5. Lynd, N. A. et al. Polydispersity and block copolymer self-assembly. *Prog. Polym. Sci.* **33**, 875–893 (2008).
6. Sides, S. W. et al. Continuous polydispersity in a self-consistent field theory for diblock copolymers. *J. Chem. Phys.* **121**, 4974–4986 (2004).
7. Lynd, N. A. et al. The role of polydispersity in the lamellar mesophase of model diblock copolymers. *J. Polym. Sci. B Polym. Phys.* **45**, 3386–3393 (2007).
8. Burger, C. et al. Polydispersity effects on the microphase-separation transition in block copolymers. *Macromolecules* **23**, 3339–3346 (1990).
9. Burger, C. et al. Polydispersity effects on the microphase-separation transition in block copolymers [Erratum to document cited in CA113(2):7140f]. *Macromolecules* **24**, 816 (1991).
10. Wolff, T. et al. Synchrotron SAXS study of the microphase separation transition in diblock copolymers. *Macromolecules* **26**, 1707–1711 (1993).
11. Widin, J. M. et al. Bulk and thin film morphological behavior of broad dispersity poly(styrene-*b*-methyl methacrylate) diblock copolymers. *Macromolecules* **46**, 4472–4480 (2013).
12. Nguyen, D. et al. Effect of ionic chain polydispersity on the size of spherical ionic microdomains in diblock ionomers. *Macromolecules* **27**, 5173–5181 (1994).
13. Rane, S. S. et al. Polydispersity index: how accurately does it measure the breath of the molecular weight distribution? *Chem. Mater.* **17**, 926 (2005).
14. Harrisson, S. The downside of dispersity: why the standard deviation is a better measure of dispersion in precision polymerization. *Polym. Chem.* **9**, 1366–1370 (2018).
15. Gilbert, R. G. et al. Dispersity in polymer science. *Pure Appl. Chem.* **81**, 351–353 (2009).
16. Carothers, W. H. Polymerization. *Chem. Rev.* **8**, 353–426 (1931).
17. Svedberg, T. Sedimentation of molecules in centrifugal fields. *Chem. Rev.* **14**, 1–15 (1934).
18. Zimm, B. H. Apparatus and methods for measurement and interpretation of the angular variation of light scattering; preliminary results on polystyrene solutions. *J. Chem. Phys.* **16**, 1099–1116 (1948).
19. Schulz, G. V. About the kinetics of chain polymerization. *Z. Physik. Chem.* **B43**, 25–46 (1939).
20. Leibler, L. Theory of microphase separation in block copolymers. *Macromolecules* **13**, 1602–1617 (1980).
21. Noro, A. et al. Effect of composition distribution on microphase-separated structure from BAB triblock copolymers. *Macromolecules* **37**, 3804–3808 (2004).
22. Matsushita, Y. et al. Molecular weight dependence of lamellar domain spacing of diblock copolymers in bulk. *Macromolecules* **23**, 4313–4316 (1990).
23. Matsushita, Y. et al. Effect of composition distribution on microphase-separated structure from diblock copolymers. *Macromolecules* **36**, 8074–8077 (2003).
24. Noro, A. et al. Effect of molecular weight distribution on microphase-separated structures from block copolymers. *Macromolecules* **38**, 4371–4376 (2005).
25. Noro, A. et al. Chain localization and interfacial thickness in microphase-separated structures of block copolymers with variable composition distributions. *Macromolecules* **39**, 7654–7661 (2006).
26. Hadziioannou, G. et al. Structural study of mixtures of styrene isoprene two- and three-block copolymers. *Macromolecules* **15**, 267–271 (1982).
27. Widin, J. M. et al. Unexpected consequences of block polydispersity on the self-assembly of ABA triblock copolymers. *J. Am. Chem. Soc.* **134**, 3834–3844 (2012).
28. Bendejacq, D. et al. Well-ordered microdomain structures in polydisperse poly(styrene)-poly(acrylic acid) diblock copolymers from controlled radical polymerization. *Macromolecules* **35**, 6645–6649 (2002).
29. Hustad, P. D. et al. Photonic polyethylene from self-assembled mesophases of polydisperse olefin block copolymers. *Macromolecules* **42**, 3788–3794 (2009).
30. Lynd, N. A. et al. Influence of polydispersity on the self-assembly of diblock copolymers. *Macromolecules* **38**, 8803–8810 (2005).
31. Lynd, N. A. et al. Effects of polydispersity on the order–disorder transition in block copolymer melts. *Macromolecules* **40**, 8050–8055 (2007).
32. Plichta, A. et al. Tuning dispersity in diblock copolymers using ARGET ATRP. *Macromol. Chem. Phys.* **213**, 2659–2668 (2012).
33. Listak, J. et al. Effect of symmetry of molecular weight distribution in block copolymers on formation of "metastable" morphologies. *Macromolecules* **41**, 5919–5927 (2008).
34. Sarbu, T. et al. Polystyrene with designed molecular weight distribution by atom transfer radical coupling. *Macromolecules* **37**, 3120–3127 (2004).
35. Weiss, E. D. et al. Atom transfer versus catalyst transfer: Deviations from ideal Poisson behavior in controlled polymerizations. *Polymer* **72**, 226–237 (2015).
36. Liu, X. et al. Polymer dispersity control by organocatalyzed living radical polymerization. *Angew. Chem. Int. Ed.* **131**, 5654–5659 (2019).
37. Li, H. et al. Tuning the molecular weight distribution atom transfer radical polymerization using deep reinforcement learning. *Mol. Syst. Des. Eng.* **3**, 496–508 (2018).
38. Meira, G. R. et al. Molecular weight distribution control in continuous "living" polymerizations through periodic operation of the monomer feed. *Polym. Eng. Sci.* **21**, 415–423 (1981).
39. Alassia, L. M. et al. Molecular weight distribution control in a semibatch living-anionic polymerization. II. Experimental study. *J. Appl. Polym. Sci.* **36**, 481–494 (1988).
40. Couso, D. A. et al. Molecular weight distribution control in a semibatch living-anionic polymerization. I. Theoretical study. *J. Appl. Polym. Sci.* **30**, 3249–3265 (1985).
41. Farkas, E. et al. Molecular weight distribution design with living polymerization reactions. *Ind. Eng. Chem. Res.* **43**, 7356–7360 (2004).
42. Meszena, Z. G. et al. Towards tailored molecular weight distributions through controlled living polymerisation reactors: a simple predictive algorithm. *Polym. React. Eng.* **71**, 71–95 (1999).
43. Seno, K. I. et al. Thermosensitive diblock copolymers with designed molecular weight distribution: Synthesis by continuous living cationic polymerization and micellization behavior. *J. Polym. Sci. A Polym. Chem.* **46**, 2212–2221 (2008).
44. Litt, M. The effects of inadequate mixing in anionic polymerization: Laminar mixing hypothesis. *J. Polym. Sci.* **58**, 429–454 (1962).
45. Gentekos, D. T. et al. Beyond dispersity: deterministic control of polymer molecular weight distribution. *J. Am. Chem. Soc.* **138**, 1848–1851 (2016).
46. Hawker, C. J. et al. New polymer synthesis by nitroxide mediated living radical polymerizations. E. *Chem. Rev.* **101**, 3661–3688 (2001).
47. Hadjichristidis, N. et al. Polymers with complex architecture by living anionic polymerization. *Chem. Rev.* **101**, 3747–3792 (2001).
48. Kottisch, V. et al. "Shaping" the future of molecular weight distributions in anionic polymerization. *ACS Macro Lett.* **5**, 796–800 (2016).
49. Corrigan, N. et al. Controlling molecular weight distributions through photoinduced flow polymerization. *Macromolecules* **50**, 8438–8448 (2017).
50. Corrigan, N. et al. Copolymers with controlled molecular weight distributions and compositional gradients through flow polymerization. *Macromolecules* **51**, 4553–4563 (2018).
51. Spinnrock, A. et al. Control of molar mass distribution by polymerization in the analytical ultracentrifuge. *Angew. Chem. Int. Ed.* **57**, 8284–8287 (2018).
52. Fredrickson, G. H. et al. Fluctuation effects in the theory of microphase separation in block copolymers. *J. Chem. Phys.* **87**, 697–705 (1987).
53. Erukhimovich, I. et al. A statistical theory of polydisperse block copolymer systems under weak supercrystallization. *Macromol. Symp.* **81**, 253–315 (1994).
54. Semenov, A. N. Contribution to the theory of microphase layering in block-copolymer melts. *Sov. Phys. JETP* **61**, 733–742 (1985).
55. Milner, S. T. et al. Effects of polydispersity in the end-grafted polymer brush. *Macromolecules* **22**, 853–861 (1989).
56. Dobrynin, A. et al. Theory of polydisperse multiblock copolymers. *Macromolecules* **30**, 4756–4765 (1997).
57. Spontak, R. J. et al. Prediction of microstructures for polydisperse block copolymers, using continuous thermodynamics. *J. Polym. Sci. B Polym. Phys.* **28**, 1379–1407 (1990).
58. Bates, F. S. et al. Block copolymers near the microphase separation transition. 3. Small-angle neutron scattering study of the homogeneous melt state. *Macromolecules* **18**, 2478–2486 (1985).
59. Mori, K. et al. Small-angle X-ray scattering from block copolymers in disordered state: 2. Effect of molecular weight distribution. *Polymer* **30**, 1389–1398 (1989).

60. Sakurai, S. et al. Evaluation of segmental interaction by small-angle X-ray scattering based on the random-phase approximation for asymmetric, polydisperse triblock copolymers. *Macromolecules* **25**, 2679–2691 (1992).
61. Wolff, T. et al. Synchrotron SAXS study of the microphase separation transition in diblock copolymers. *Macromolecules* **26**, 1707–1711 (1993).
62. Cooke, D. M. et al. Effects of polydispersity on phase behavior of diblock copolymers. *Macromolecules* **39**, 6661–6671 (2006).
63. Lynd, N. A. et al. Theory of polydisperse block copolymer melts: beyond the Schulz–Zimm distribution. *Macromolecules* **41**, 4531–4533 (2008).
64. Matsen, M. W. Effect of large degrees of polydispersity on strongly segregated block copolymers. *Eur. Phys. J. E Soft Matter Biol. Phys.* **21**, 199–207 (2006).
65. Woo, S. et al. Domain swelling in ARB-type triblock copolymers via self-adjusting effective dispersity. *Soft Matter* **13**, 5527–5534 (2017).
66. Broseta, D. et al. Molecular weight and polydispersity effects at polymer-polymer interfaces. *Macromolecules* **23**, 132–139 (1990).
67. Fredrickson, G. H. et al. Theory of polydisperse inhomogeneous polymers. *Macromolecules* **36**, 5415–5423 (2003).
68. Matsen, M. W. Phase behavior of block copolymer/homopolymer blends. *Macromolecules* **28**, 5765–5773 (1995).
69. Loo, Y.-L. A highly regular hexagonally perforated lamellar structure in a quiescent diblock copolymer. *Macromolecules* **38**, 4947–4949 (2005).
70. Hashimoto, T. et al. Observation of "mesh" and "strut" structures in block copolymer/homopolymer mixtures. *Macromolecules* **25**, 1433–1439 (1992).
71. Hajduk, D. A. et al. Stability of the perforated layer (PL) phase in diblock copolymer melts. *Macromolecules* **30**, 3788–3795 (1997).
72. Matsen, M. W. Polydispersity-induced macrophase separation in diblock copolymer melts. *Phys. Rev. Lett.* **99**, 148304 (2007).
73. Matsen, M. W. et al. Unifying weak- and strong-segregation block copolymer theories. *Macromolecules* **29**, 1091–1098 (1996).
74. Matsen, M. W. et al. Origins of complex self-assembly in block copolymers. *Macromolecules* **29**, 7641–7644 (1996).
75. Gentekos, D. T. et al. Exploiting molecular weight distribution shape to tune domain spacing in block copolymer thin films. *J. Am. Chem. Soc.* **140**, 4639–4648 (2018).
76. Busch, P. et al. Lamellar diblock copolymer thin films investigated by tapping mode atomic force microscopy: Molar-mass dependence of surface ordering. *Macromolecules* **36**, 8717–8727 (2003).
77. Gentekos, D. T. et al. Molecular weight distribution shape as a versatile approach to tailoring block copolymer phase behavior. *ACS Macro Lett.* **7**, 677–682 (2018).
78. Pao, Y. H. Dependence of intrinsic viscosity of dilute solutions of macromolecules on velocity gradient. *J. Chem. Phys.* **25**, 1294–1295 (1956).
79. Bueche, F. Influence of rate of shear on the apparent viscosity of A—dilute polymer solutions, and B—bulk polymers. *J. Chem. Phys.* **22**, 1570–1576 (1954).
80. Rouse, P. E. A theory of the linear viscoelastic properties of dilute solutions of coiling polymers. *J. Chem. Phys.* **21**, 1272–1280 (1953).
81. Pao, Y. H. Hydrodynamic theory for the flow of a viscoelastic fluid. *J. Appl. Phys.* **28**, 591–598 (1957).
82. Graessley, W. W. Molecular entanglement theory of flow behavior in amorphous polymers. *J. Chem. Phys.* **43**, 2696–2703 (1965).
83. Dunleavy, J. E. et al. Correlation of shear behavior of solutions of polyisobutylene. *Trans. Soc. Rheol.* **10**, 157–168 (1966).
84. Bremner, T. et al. Melt flow index values and molecular weight distributions of commercial thermoplastics. *J. Appl. Poly. Sci.* **41**, 1617–1627 (1990).
85. Rodríguez-Hernández, M. T. et al. Determination of the molecular characteristics of commercial polyethylenes with different architectures and the relation with the melt flow index. *J. Appl. Poly. Sci.* **104**, 1572–1578 (2007).
86. Utracki, L. A. et al. Linear low density polyethylenes and their blends: Part 2. Shear flow of LLDPE's. *Polym. Eng. Sci.* **27**, 367–379 (1987).
87. Aho, J. et al. Rheology as a tool for evaluation of melt processability of innovative dosage forms. *Int. J. Pharm.* **494**, 623–642 (2015).
88. Ansari, M. et al. Rheology of Ziegler–Natta and metallocene high-density polyethylenes: broad molecular weight distribution effects. *Rheol. Acta* **50**, 17–27 (2011).
89. Ballman, R. L. et al. The influence of molecular weight distribution on some properties of polystyrene melt. *J. Polym. Sci. A Gen. Papers* **2**, 3557–3575 (1964).
90. Middleman, S. Effect of molecular weight distribution on viscosity of polymeric fluids. *J. Appl. Poly. Sci.* **11**, 417–424 (1967).
91. Colby, R. H. et al. The melt viscosity-molecular weight relationship for linear polymers. *Macromol.* **20**, 2226–2237 (1987).
92. Cross, M. M. Rheology of non-Newtonian fluids: a new flow equation for pseudoplastic systems. *J. Colloid. Sci.* **20**, 417–437 (1965).
93. Des Cloiseaux, J. Double reptation vs. simple reptation in polymer melts. *Europhys. Lett.* **5**, 437–442 (1988).
94. Gloor, W. E. The numerical evaluation of parameters in distribution functions of polymers from their molecular weight distributions. *J. Appl. Polym. Sci.* **22**, 1177–1182 (1978).
95. Nichetti, D. et al. Viscosity model for polydisperse polymer melts. *J. Rheol.* **42**, 951–969 (1998).
96. Rudd, J. The effect of molecular weight distribution on the rheological properties of polystyrene. *J. Polym. Sci. A Polym. Chem.* **44**, 459–474 (1960).
97. González-González, V. A. et al. Polypropylene chain scissions and molecular weight changes in multiple extrusion. *Polym. Degrad. Stab.* **60**, 33–42 (1998).
98. Wasserman, S. H. et al. Effects of polydispersity on linear viscoelasticity in entangled polymer melts. *J. Rheol.* **36**, 543–572 (1992).
99. Stürzel, M. et al. From multisite polymerization catalysis to sustainable materials and all-polyolefin composites. *Chem. Rev.* **116**, 1398–1433 (2016).
100. Nadgorny, M. et al. Manipulation of molecular weight distribution shape as a new strategy to control processing parameters. *Macromol. Rapid. Commun.* **38**, 1700352 (2017).
101. Rubber industry sees value in MWD. *Chem. Eng. News Archive* **43**, 40–41 (1965).
102. Fink, Y. et al. Block copolymers as photonic bandgap materials. *J. Lightwave Technol.* **17**, 1963–1969 (1999).
103. Stefik, M. et al. Block copolymer self-assembly for nanophotonics. *Chem. Soc. Rev.* **44**, 5076–5091 (2015).
104. Kang, Y. et al. Broad-wavelength-range chemically tunable block-copolymer photonic gels. *Nat. Mater.* **6**, 957–960 (2007).
105. Kang, C. et al. Full color stop bands in hybrid organic/inorganic block copolymer photonic gels by swelling-freezing. *J. Am. Chem. Soc.* **131**, 7538–7539 (2009).
106. Urbas, A. M. et al. Bicontinuous cubic block copolymer photonic crystals. *Adv. Mater.* **14**, 1850–1853 (2002).
107. Park, M. et al. Block copolymer lithography: periodic arrays of $\sim 10^{11}$ holes in 1 square centimeter. *Science* **276**, 1401–1404 (1997).
108. Honeker, C. C. et al. Impact of morphological orientation in determining mechanical properties in triblock copolymer systems. *Chem. Mater.* **8**, 1702–1714 (1996).
109. Bang, J. et al. Block copolymer nanolithography: translation of molecular level control to nanoscale patterns. *Adv. Mater.* **21**, 4769–4792 (2009).
110. Ruiz, R. et al. Density multiplication and improved lithography by directed block copolymer assembly. *Science* **321**, 936–939 (2008).
111. Kim, S. O. et al. Epitaxial self-assembly of block copolymers on lithographically defined nanopatterned substrates. *Nature* **424**, 411–414 (2003).
112. Chen, L. et al. Robust nanoporous membranes templated by a doubly reactive block copolymer. *J. Am. Chem. Soc.* **129**, 13786–13787 (2007).
113. Quirk, R. et al. in *Thermoplastic Elastomers* 2nd edn (eds Holden, G. et al.) 72–100 (Hanser Publishers, 1996).
114. Jackson, E. A. et al. Nanoporous membranes derived from block copolymers; from drug delivery to water filtration. *ACS Nano* **4**, 3548–3553 (2010).
115. Ahn, H. et al. Nanoporous block copolymer membranes for ultrafiltration: a simple approach to size tunability. *ACS Nano* **8**, 11745–11752 (2014).
116. Zhao, D. et al. Triblock copolymer syntheses of mesoporous silica with periodic 50 to 300 angstrom pores. *Science* **279**, 548–552 (1998).
117. Liang, C. et al. Synthesis of a large-scale highly ordered porous carbon film by self-assembly of block copolymers. *Angew. Chem. Int. Ed.* **43**, 5785–5789 (2004).
118. Jeong, B. et al. Biodegradable block copolymers as injectable drug-delivery systems. *Nature* **388**, 860–862 (1997).
119. Kataoka, K. et al. Block copolymer micelles for drug delivery: design, characterization and biological significance. *Adv. Drug Deliv. Rev.* **64**, 37–48 (2012).
120. Fischer, W. et al. Anionic polymerization process. US6444762 B1 (1997).
121. Wyatt, P. J. Light scattering and the absolute characterization of macromolecules. *Anal. Chim. Acta.* **272**, 1–40 (1993).
122. Lange, H. et al. Gel permeation chromatography in determining molecular weights of lignins: critical aspects revisited for improved utility in the development of novel materials. *ACS Sustain. Chem. Eng.* **4**, 5167–5180 (2016).
123. Determann, H. in *Gel Chromatography · Gel Filtration · Gel Permeation. · Molecular Sieves, A Laboratory Handbook* 2nd edn (Springer, 1969).
124. Matyjaszewski, K. et al. Atom transfer radical polymerization. *Chem. Rev.* **101**, 2921–2990 (2001).
125. Flory, P. J. Molecular size distribution in linear condensation polymers. *J. Am. Chem. Soc.* **58**, 1877–1885 (1936).
126. Ryu, J. et al. Molecular weight distribution of branched polystyrene: Propagation of Poisson distribution. *Macromolecules* **37**, 8805–8807 (2004).
127. Peebles, L. H., Jr. in *Molecular Weight Distributions in Polymers* (Interscience, 1971).
128. Rudin, A. Molecular weight distributions of polymers. *J. Chem. Educ.* **46**, 595 (1969).
129. Gong, X. et al. Molecular weight distribution characteristics (of a polymer) derived from a stretched-exponential PGSTE NMR response function—simulation. *Macromol. Chem. Phys.* **213**, 278–284 (2012).
130. Chem, S.-A. et al. The skewness of polymer molecular weight distributions. *J. Polym. Sci. Polym. Chem. Ed.* **21**, 3373–3380 (1983).
131. Kirkland, J. J. et al. Sampling and extra-column effects in high-performance liquid chromatography; influence of peak skew on plate count calculations. *J. Chromatogr. Sci.* **15**, 303–316 (1977).

Acknowledgements
The authors acknowledge the Cornell Center for Materials Research (CCMR) through the National Science Foundation (NSF) Materials Research Science and Engineering Centers (MRSEC) program (DMR-1719875). B.P.F. thanks 3M and the Sloan Foundation for partially supporting this work.

Author Contributions
All authors contributed to the discussion and writing of this manuscript.

Competing Interests
The authors declare no competing interests.

Publisher's note
Springer Nature remains neutral with regard to jurisdictional claims in published maps and institutional affiliations.